

Broadband Low Residual Amplitude Modulation Phase Modulator Arrays for Optical Beamsteering Applications

Michael Nickerson^{1*}, Bowen Song¹, Lei Wang¹, Paul Verrinder¹, Jim Brookhyser², Gregory Erwin², Jan Kleinert², and Jonathan Klamkin¹

¹Department of Electrical and Computer Engineering, University of California, Santa Barbara, CA 93106, USA

²MKS Instruments, Equipment & Solutions Division, 14523 SW Millikan Way, Beaverton, OR 97005, USA

*nickersonm@ece.ucsb.edu

Abstract: Low loss phase modulator arrays with 1x16 splitters are demonstrated on a gallium arsenide platform that is suitable for monolithic integration with gain. The modulators demonstrated a $V_{\pi}L$ efficiency of 0.7 V·cm at 1030 nm. © 2022 The Author(s)

1. Introduction

Optical phased arrays (OPAs) are a promising solution for solid-state beam steering with applications ranging from terrestrial LIDAR to free-space optical communication and optical switching [1]. Photonic integrated circuit (PIC) technology is critical for reducing the size, weight, and power of OPAs. Silicon photonics (SiPh) and lithium niobate (LN) have been investigated for OPAs operating at 1550 nm [2], but challenges remain for practical LIDAR systems due to the lack of integrated laser sources and efficient modulators with low residual amplitude modulation (RAM). SiPh is also incompatible with near-1 μm laser wavelengths that are commonly used in remote LIDAR sensing spectrometry [3], offer compatibility with existing topographical LIDAR systems, and are amenable to efficient fiber amplification. Group III-V semiconductor PICs offer integrated lasers, optical amplification, and efficient low RAM optical phase modulators at many wavelengths, providing a promising platform for monolithically integrated OPAs.

In this work, a gallium arsenide (GaAs) PIC with a single input and an array of 16 phase modulators is presented for use in OPA applications. Cascaded 1x4 multi-mode interference (MMI) couplers provide a compact beam splitter. Individual 4-mm-long modulators demonstrate $V_{\pi}L$ of 0.7 V·cm at 1030 nm, RAM under 0.5 dB below 7π modulation, DC power consumption less than 200 nW per modulator, and estimated RC-limited 2 GHz modulation bandwidth. This GaAs based PIC platform is suitable for direct integration with on-chip laser sources near 1 μm [4], demonstrating the potential for a fully monolithically integrated OPA.

2. Device Design and Fabrication

Cross sections of the GaAs PIC components are shown in Figure 1(a). Deep ridge waveguides were fabricated with a Cl_2/N_2 dry etch, and modulators were formed by depositing P-contacts on top of waveguides, with N-contacts placed nearby on the highly n-doped GaAs buffer layer. A reverse-biased P-p-i-n-N double heterostructure design was implemented to reduce RAM and insertion loss. The design yields high overlap between a nearly linear electric field and the optical mode to utilize linear and quadratic electro-optic effects. Low optical absorption is achieved by a graded-index structure providing >95% overlap between the optical field and the guiding intrinsic GaAs region.

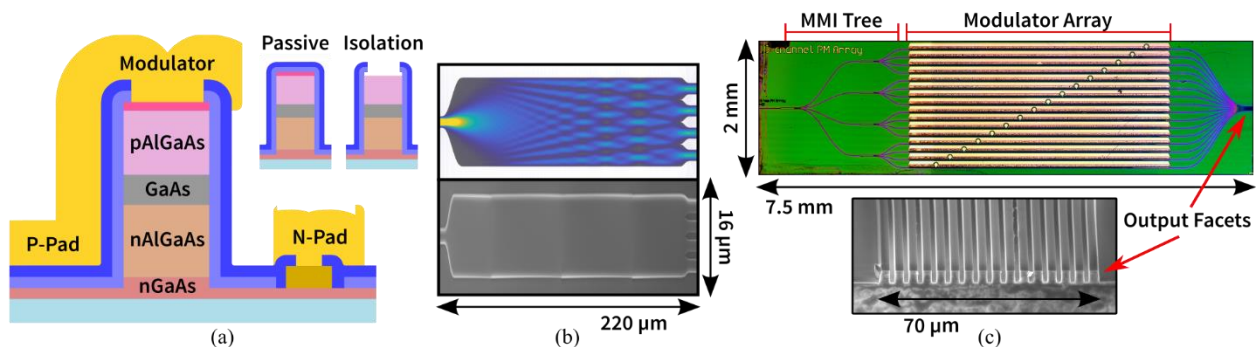


Figure 1. (a) Cross-section schematic of waveguide structures. (b) Simulation and SEM image of 1x4 MMI. (c) Optical micrograph of fabricated PIC and inclined SEM image of AR coated output facets.

To effect longitudinal electrical isolation between modulators and passive components, the top p-GaAs layer is removed from short segments on either end of the modulators. Passive waveguides simply omit the metal contacts. Several 1x4 MMIs are cascaded to form the 1x16 splitter; Figure 1(b) shows the simulated and fabricated versions. The output of 16 parallel phase modulators is collapsed to a dense 4 μm pitch, suitable for an optical phased array

with $2 \sin^{-1}(\lambda/2d) = 14^\circ$ grating lobe free steering range. The fabricated PIC shown in Figure 1(c) has a footprint of 7.5 mm x 2 mm. Channel count is currently limited by in-house packaging constraints, but is easily scalable.

3. Measurement Results

Multiple PICs and other test structures were measured via edge coupling to lensed fibers. Packaged 980 nm and 1030 nm DFB lasers and a tunable O-band laser were used as light sources. Modulation response of individual 4 mm devices was determined by fitting single-sided Mach-Zehnder modulator (MZM) transmission, shown in Figure 2(a). At 1030 nm, the best fit across 15 separate measurements was $\Delta\phi(V_{bias}) = (26^\circ/\text{mm}) \cdot V_{bias} + (0.4^\circ/\text{mm}) \cdot V_{bias}^2$, corresponding to modulation efficiency of 0.6 V·cm for a 4 mm device. Modulation was tested across a range of wavelengths from 980 nm to 1360 nm (Fig. 2(b)). With single-sided V_{π} -L better than 1.22 V·cm over 380 nm of bandwidth, these devices are significantly more efficient than most LN and low-RAM SiPh phase modulators [2].

Modulator RAM was characterized by MZM fringe peaks and is under 0.5 dB until the onset of Franz-Keldysh electroabsorption. Equipment limitations precluded reaching the electroabsorption onset near 1300 nm. Figure 2(c) is a parametric plot of RAM and modulation depth, both values being functions of bias and wavelength.

DC leakage currents of 4 mm devices are as small as 50 nA at -5 V bias (3π modulation), corresponding to DC power usage under 200 nW per modulator. Equipment limitations currently prevent measurement of power and modulation bandwidth above DC and 1 MHz respectively, but electrical testing of the 4 mm modulators determined 7 pF junction plus parasitic capacitance and 10 Ω series resistance.

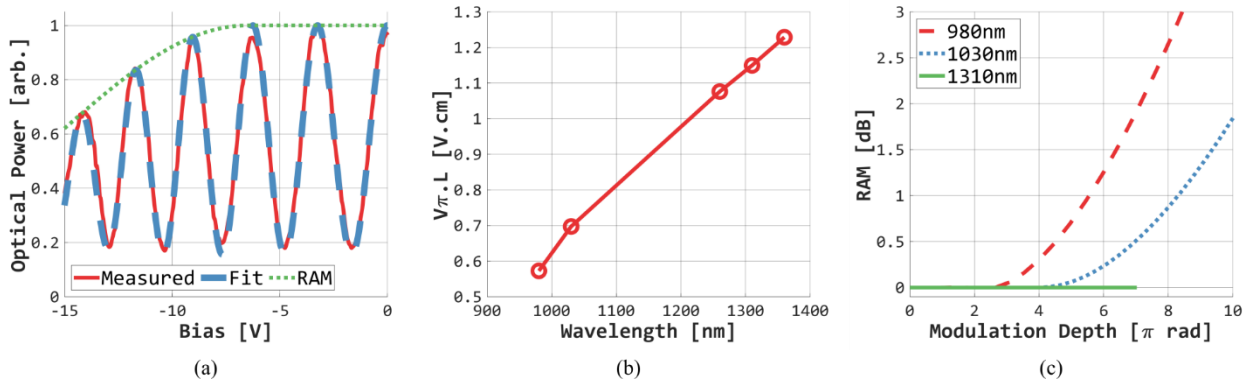


Figure 2. (a) Measurement and fit of single-sided MZM transmission as bias voltage is varied. (b) 4 mm modulator efficiency at various wavelengths. (c) Interaction of RAM and modulation depth for a 4 mm device; both are functions of applied bias, which is equipment limited.

4. Conclusion

GaAs PICs including passive splitters and low-RAM phase modulators have been developed, and a 16-channel device suitable for use as an OPA was fabricated. Individual modulators demonstrated V_{π} -L modulation efficiency of 0.7 V·cm at 1030 nm, with broadband operation measured from 980 nm to 1360 nm. Including a dense waveguide array output and an epitaxy compatible with gain in the same wavelength range, these PICs demonstrate the potential for a fully monolithically integrated OPA with no external optical components.

5. Acknowledgements

The authors acknowledge funding support from MKS Instruments. A portion of this work was performed in the UCSB Nanofabrication Facility, an open access laboratory.

6. References

- [1] C. V. Poulton *et al.*, “Long-Range LiDAR and Free-Space Data Communication with High-Performance Optical Phased Arrays,” *IEEE J. Sel. Top. Quantum Electron.*, pp. 1–1, 2019. <https://doi.org/10/gfx8d3>
- [2] M. Zhang, C. Wang, P. Kharel, D. Zhu, and M. Lončar, “Integrated lithium niobate electro-optic modulators: when performance meets scalability,” *Optica*, vol. 8, no. 5, pp. 652–667, Optical Society of America, May 2021. <https://doi.org/10/gj47x3>
- [3] J. Fridlander *et al.*, “Dual Laser Indium Phosphide Photonic Integrated Circuit for Integrated Path Differential Absorption Lidar,” *IEEE J. Sel. Top. Quantum Electron.*, vol. 28, no. 1, pp. 1–8, Jan. 2022. <https://doi.org/10/gmzfnf>
- [4] P. A. Verrinder *et al.*, “Gallium Arsenide Photonic Integrated Circuit Platform for Tunable Laser Applications,” *IEEE J. Sel. Top. Quantum Electron.*, vol. 28, no. 1, pp. 1–9, Jan. 2022. <https://doi.org/10/gmzfnf>